RSC Advances

ROYAL SOCIETY OF CHEMISTRY

www.rsc.org/advances

Si nanocorals/PbS quantum dots composited high efficiency c-Si solar cell

Wuliang Feng, Jie Liu, Yusheng Li, Jie Liang, Xibin Yu*

The Education Ministry Key Lab of Resource Chemistry and Shanghai Key Laboratory of Rare Earth Functional Materials, Department of Chemistry, Shanghai Normal University, Shanghai 200234, People's Republic of China.

*Address correspondence to：xibinyu@shnu.edu.cn

Keywords: Solar Cell, Silicon, Nanocorads, PbS, Quantum Dots

Abstract

A composited colloidal Si nanocorals (NCs)/ PbS quantum dots (QDs) p-n active layer was demonstrated to have the potential to reduce the surface recombination velocity and further improve the cell efficiency, not only due to the light trapping structure of Si NCs, but the ability of passivation as well as down-conversion in PbS QDs. Appropriate length of Si NCs was acquired first by investigating the interaction of light absorption and effective minority-carrier lifetime. After the integration with PbS QDs, the composited solar cell showed a 30% increase in power conversion efficiency (PCE), compared to its bare Si substrate counterpart. Thus, we believe that the Si NCs and PbS QDs composited structure is promising to enhance the PCE of the Si based photovoltaic device nowadays.

1. Introduction

Silicon based photovoltaic devices take over 80% of solar cell market due to its earth abundant, high efficiency, and maturity in fabrication at large scale. According to Shockley-Queisser theory, the efficiency of standard crystalline silicon (c-Si) solar cell used today is limited to 31%.[1] Optical, recombination, series resistance, and thermal or quantum losses are the four main losses that lead to the reduction of the Si solar cell efficiency.[2]

Polished Si substrate is a poor absorber that reflects approximately 35% of incident photons. To reduce optical losses, different kinds of surface texturing and antireflection layers (AR) have been carried out in commercial scale. Such processes have achieved the reflectance of incident photons to <10%. However, UV light is still highly reflected, which accounts for ~7% of spectral irradiance.[3, 4] Moreover, plasma enhanced chemical vapor deposition (PECVD) is used to deposit AR coating in large area, but this process is a costlier one. By contrast, sub-wavelength Si nanostructures can provide remarkable diffuse reflection and are low-cost in fabrication. When the Si nanostructures decrease to quantum scale (<7nm), the greater split of the Fermi levels will probably increase V_{oc}.[5] Despite of the benefits from light trapping, the high surface recombination velocity caused by surface defects is the main obstacle for the development of the 1-D sub-wavelength structure Si solar cell.[6, 7]

Crystalline silicon is an indirect-bandgap semiconductor with bandgap of 1.12 eV, absorption of high-energy photons creates hot electrons and holes that cool quickly to the band edges by sequential emission of phonons. Approximately half of the solar energy loss is related to the spectral mismatch, known as thermal or quantum losses. The utility of the whole solar spectrum can be improved by using a certain down-conversion materials, due to the extension of operating spectral range toward ultraviolet and emit lower energy photons. Rare earth-doped luminescent materials have been extensively studied and have been demonstrated as prominent down-conversion property in recent decades.[8, 9] However, the integration of such materials on Si based solar cell is still far from practical. But apart from that, inorganic semiconductor quantum dots (QDs) also possess down-conversion property to improve the utility of the full solar energy. Inorganic QDs have the possibility of harvesting effective UV

light then emitted via photon down-conversion, due to the absorption of high-energy photon converted into two photons with lower energies.[10-13] Additional benefit from the QDs comes from the ability to slow down electronic relaxation.[14, 15] The extraction of hot carriers before they cool to the band edges will acquire high efficiency solar cells. The great interest of QDs also arose from the Multiple exciton generation (MEG) phenomenon, a process that absorption of a photon exceeds twice the bandgap energy to produce two or more electron-hole pairs. If all of the energy of the hot carriers were captured, solar-to-electric power conversion efficiencies could be theoretically increased to as high as 66%.[16-19] With the prominent photoelectric properties, QDs will open up a way toward breaking the single junction Shockley-Queisser limit of the first and second generation solar cells, thus moving photovoltaic cells toward the third generation regime.[18]

Here, Si coral like one-dimensional (1-D) nanostructure was synthesised. We investigated how this Si nanocorals (NCs) affected the photovoltaic performance of single crystalline p–n homojunction Si solar cell with a pyramid textured surface, and its integration with PbS QDs afterwards. Firstly, optimum length of 1-D Si NCs was explored. The 1-D light trapping structure successfully decreased the reflectance of UV-VIS-NIR light to <10% and increased PCE by 17.5%. Subsequently, ~3nm zero-dimension (0-D) PbS QDs were deposited on Si NCs by spin-coating. After the Si NCs solar cell is integrated with PbS QDs, the composited solar cell showed a further enhancement of 10.7% in PCE. It means that a total 30% enhancement of PCE is achieved compared to the pyramid textured Si without Si NCs and PbS QDs. Based on the superior photoelectric performance, we demonstrate that the 0-D/1-D structure composited solar cell with the properties of superior light trapping, photo down-conversion and remarkable passivation will have a chance to improve the current c-Si based solar cell.

2. Experimental

2.1 Growth of vertically aligned Si NCs.

The pyramid textured single-crystalline Si wafers employed in this work were purchased from Changzhou Yijing Optoelectronics Technology Co., Ltd. The thickness of wafers was 200 μm with bulk p-n junction, the resistivity of Si wafer is in the range of 1-10Ω cm. Vertically aligned Si NCs were prepared using metal-assisted electroless etching (MAE) by two steps.[20-22] Firstly, the pyramid textured silicon substrate was etched in an aqueous solution of silver nitrate (0.002 M) and hydrofluoric acid (0.4 M) for 30s to deposit a layer of Ag nanoparticle masks. Then, the pyramid textured silicon substrate with Ag nanoparticle masks was immersed into an aqueous solution of hydrogenperoxide (0.7 M), hydrofluoric acid (0.4 M) for 0, 15s, 30s, 45s, 60s to grow Si NCs on the n-type surface. The length of Si NCs was adjusted by changing etching times. The pyramid textured Si substrate with Si NCs was then washed with concentrated nitric acid for 5-10 min to completely remove residual silver masks and dried under air. All the MAE processes were operated at room temperature.

2.2 Synthesis of PbS QDs.

The PbS QDs were prepared by wet solution phase chemical syntheses with some modifications.[23] In brief, 910 mg of lead acetate was dissolved in 8 mL of oleylamine, reacted under N_2 gas at 150 °C for 40 min to form the Pb-oleylamine complex. Afterward, 6 mL of oleic acid solution containing 115 mg of sulfur were quickly injected into the above reaction solution. The resulting mixture was heated to 200 °C and kept for 30 min. After the solution was cooled to room temperature, hexane was added to precipitate PbS QDs followed by centrifugation. The solid product dispersed very well in toluene.

2.3 Characterization.

Field emission scanning electron microscopic (FESEM, Hitachi, Japan, operated at 15 kV) was used to observe the cross-section of the sample. A JEOL JEM-200CX microscope operating at 160 kV in the bright-field mode was used for transmission electron microscopy (TEM), to characterize PbS QDs. X-ray diffraction (XRD) patterns was recorded by D/MAX-2000 (Rigaku, Japan), using Cu-Kα radiation at a scan rate (2θ) of 2° min−1. The absorption and reflection spectra of the specimens were measured using CARY 500 Scan UV/VIS/NIR spectrophotometer with an integrating sphere (Labsphere) in a wavelength range of 250-1200 nm. The effective recombination minority-carrier lifetime of the specimens

were characterized by Semilab WT-2000PVN. Photoluminescence spectroscopy was carried out with a VARIAN Cary-Eclipse 500 fluorescence spectrophotometer equipped with a 60 W Xenon lamp as the excitation source, the sample was excited by a light beam with 650 nm. The absorption spectra of PbS QDs was characterized by Beckman Coulter DU 730 UV/VIS/NIR spectrophotometer. The total cell area measured is 9 cm. Chemical vapor deposition (CVD) is employed to evaporation Al as backside electrode. Frontside Ag electrode is printed and dried at 120 °C, and went through rapid thermal annealing at 750 °C for 2s. The J-V characteristics of the solar cells were investigated under the illumination of AM1.5G (100 mW/cm^2) and provided with Zennium electrochemical workstation (model: Xpot). The light intensity was calibrated with a silicon standard cell.

3. Results and discussion

1-D Si nanocorals are grown on the pyramid textured Si surface to improve the absorptive character. Previous studies of Si sub-wavelength structures are mainly based on p-type buke Si. The p-type 1-D structure can grown to be micron-sized, then converted to be n-type afterwards.[24] But Si NCs in this length would be harmful in our system, since the thickness of the bulk n-type Si is no more than 1μm. Fig. 1 shows the surface and cross sectional FESEM images of Si NCs of 20 nm, 80 nm, 120 nm and 200 nm, corresponding to the electro-less etching time of 15 s, 30 s, 45 s and 60 s in the aqueous solution of H_2O_2 & HF, respectively. The diameter of Si NCs increases with the increase of etching time. The absorption spectra of Si NCs are shown in Fig. 2a. It is found that the absorbance in 250-1100 nm reinforced rapidly with the increase of Si NCs length. The absorption spectrum of pyramid textured Si without NCs is displayed as line a. Even though the absorption spectrum has been broadened when the polished Si is pyramid textured. The absorbance in the region of 250-550 nm is still low. Interestingly, as the effect of Si NCs, the absorbance between 250-550 nm is greatly improved. This is because high-energy photons have larger absorption coefficient on silicon surface than low-energy photons, absorption depth is given by the inverse of the absorption coefficient, or α^{-1}. Presumably, high-energy photons tend to have shallower absorption depth.[7] As the increase of the superficial area on Si NCs, more high-energy photons are absorbed, leading to the expansion of absorption spectrum to UV region.

Regardless of the light trapping benefits from the 1-D Si NCs, the surface recombination velocity will have a negative effect on J_{sc} at the same time. In general, recombination loss depends on the surface defect of Si NCs that restricts the cell conversion efficiency. Si NCs arrays with high aspect ratios have large surface recombination velocity, leading to poor charge carrier collection efficiency. The effective minority-carrier recombination lifetime and absorbance as a function of the length of Si NCs are shown in Fig. 2b. The absorption increase is directly proportional to the length of Si NCs. Meanwhile, the recombination lifetime decreases rapidly with the length increase of Si NCs. This will probably decrease J_{sc}, indicating that the recombination lifetime of minority-carrier is inversely proportional to the surface recombination velocity, and J_{sc} is square root proportional to the minority-carrier recombination lifetime. As the negative correlation displayed between light absorption and minority-carrier recombination lifetime, J_{sc} would peak at a specific length of Si NCs.

The photoelectric performances of Si solar cell with Si NCs of different lengths (0, 20, 80, 120, 200 nm) are investigated under the illumination of AM1.5G. The photovoltaic performance indicated by J_{sc}, V_{oc}, FF, and PCE as a function of Si NCs length is estimated and plotted in Fig. 2d. The largest J_{sc} value (30.07 mA/cm^2) is achieved by a Si NCs solar cell with 80nm long Si NCs, which is a 14.7% enhancement, compared to J_{sc} value of the pyramid textured surface without Si NCs (26.22 mA/cm^2). The J-V characteristic of Si solar cell with 80nm NCs is shown in Fig. 2c. Even though the absorbance of 80 nm long Si NCs is 45% stronger than that of the non Si NCs counterpart, the absorption enhancement occur mostly in the region of 250-550nm, where photon energy is quickly lost due to the surface recombination. Thus, we believe that the optical benefit is counteracted by the enhanced recombination velocity to a certain extent. When the length of Si NCs comes to 200 nm, J_{sc} rapidly decreases to 23.25 mA/cm^2. This indicates that the enhanced recombination velocity dominates over the optical benefit, leading to an inferiored J_{sc}. The open-circuit voltage (V_{oc}) exhibits negligible change. The Si NCs in our work have exceeded the Si Bohr radius, so they do not change the Fermi energy distribution in the p-n junction of the Si solar cell. Similarly, an ignorable change of FF indicates that Si NCs on the top of the device do not affect the series resistance. In this case, the PEC would be mainly influenced by J_{sc} rather than V_{oc} or FF since J_{sc} of the Si NCs is directly influenced by the interaction of the minority carrier lifetime and light absorption. As the curves displayed in the graph, PCE has an analogous changing trend with J_{sc}, peaks at 80 nm. It increases from 9.49% to 11.15%, indicating that the enhanced absorbance greatly dominates over surface recombination.

Based on the considerable enhancement of J_{sc} and PCE as Si NCs are employed on the pyramid textured surface, the PCE still remain great potential to be further improved, which lies in the reduction of surface recombination velocity. Thus, we studied the influence of PbS QDs integrated on Si NCs solar cell. Lead sulfide has a large Bohr radius (18 nm) with certain down-conversion depending on the size, making it a promising candidate for high efficient photovoltaic devices. TEM image (Fig. 4a) shows that the PbS QDs are uniform and mono-disperse with an average diameter of 2~3 nm. PbS QDs are spin coated on the Si NCs (2000r/min) and then thermal treated under 200□ with the protection of N_2 for 7 min, to obtain a close contact between PbS & Si NCs. This process is important to prevent extra series resistance. Schematic illustration of Si NCs/PbS QDs composited solar cell is shown in Fig. 3. The length of Si NCs employed is 80nm. The complex light-trapping structure with rough surface is in propitious to the deposition of PbS QDs. As shown in Fig. 4b, the thickness of the Si NCs capped with PbS layer is about 100 nm and PbS QDs are

well-distributed, indicating that a large amount of PbS QDs are padded in the gap of Si NCs and a ~20 nm PbS QDs layer is on the topside. The XRD pattern of PbS QDs integrated with Si NCs is shown in Fig. 4c. The peak at 2θ value of 69.130° can be indexed to the (400) plane of Si. The diffraction peak of Si overwhelmed the diffraction peak of PbS because of the ultra small amount of PbS, compared to Si substrate. As shown in Figure 4c (2), the peak at 2θ values of 25.963°, 30.074°, 43.058°, 50.976°, 53.411° can be indexed to the (111) , (200), (220), (311), (222) planes of PbS, indicating that the pure phase of PbS was obtained and no other impurity peaks were detected.

Fig. 2c shows the J-V characteristic of pyramid textured Si without Si NCs, pyramid textured Si with 80 nm NCs, and the composited solar cell. The photoelectric performance is summarized in Tab. 1. It is well worth noting that the V_{oc} displays a slightly enhancement after integrated with PbS QDs. This is probably due to the additional light trapping of PbS QDs on the top of the device. The generation of electron-hole pairs is increased, leading to the slight change of the Fermi energy distribution in the Si p-n junction.[25] Another observation of the J-V characteristic obtained from the slope of the curves indicates that the FF of the composited solar cell stays almost unchanged. It implies that PbS QDs on the top side of the cell do not affect the conductance of electrons in the n^+ emitter layer and no extra series resistance produced. The J_{sc} of PbS/Si NCs increased from 30.07 to 32.76 mA/cm^2. With both the enhancement of V_{oc} and J_{sc}, the PCE of the composited solar cell exhibits a 10.7% improvement, compared to its non PbS capped Si NCs counterpart.

In order to understand the underlying mechanism for the further enhanced cell efficiency, we studied the effective recombination minority-carrier lifetime of Si NCs capped with PbS QDs. As shown in Fig. 5a, after integrated with PbS QDs, the effective recombination minority-carrier lifetime of Si NCs is remarkably improved, which corresponds to the considerable enhancement of J_{sc}. Implying the PbS QDs coating on the topside act as a passivation layer. In the previous reports, PbS QDs have the ability to slow down electronic relaxation.[26] As the quasi-continuous valence and conduction bands of the bulk semiconductor are discretized in PbS QDs, due to the confinement of charge carriers. The energy spacing between the electronic levels becomes much larger than the highest phonon frequency of the lattice, resulting in a “phonon bottleneck”. Thus, hot carrier relaxation is only possible via slower multi phonon emission.[15] With the ability to slow down electronic relaxation, PbS QDs achieve a fast extraction of hot carriers before they cool to the band edges, which is directly contributed to the enhancement of minority-carrier lifetime. In

addition, previous reports indicated that the MEG character of PbS QDs would help to generate more electron-hole pairs.[27] On the macroscopic circumstance, the higher density of hot carriers enhanced the effective recombination minority-carrier lifetime to some extent. Typically, hot electron-hole pairs generated in bulk c-Si by high energy photons relax rapidly to the conduction and valence band edage, losing the excess energy by thermalization. With MEG, the excess energy of high energy photons is converted to additional excitons, enhancing the J_{sc}. Moreover, it is interesting to find that the recombination lifetime difference between Si NCs and Si NCs capped with PbS QDs increases with the increase of Si NCs length. The enhancements by Si NCs capped with PbS QDs are 2.4%, 7.8%, 11.3%, 19.9%, and 41.5% for Si NCs with a length of 0, 20, 80, 120, and 200 nm, respectively. This variation tendency is probably due to the bigger recombination velocity of the longer Si NCs. Even though the recombination lifetimes of 120 nm and 200 nm Si NCs capped with PbS QDs achieved much improvement, their cell efficiencies were 11.76% and 10.52%, respectively, which are lower than that of PbS QDs /80 nm Si NCs composited cell.

To investigate the down-conversion property of PbS QDs, the absorption and photoluminescence (PL) spectra are shown in Fig. 5b. The absorption peak of PbS QDs is observed at 685 nm. With an band gap of 1.81 eV, the size of PbS QDs is measured to be 2.5 nm based on the Potential Morphing Method (PMM), which is quite correspondence with previous reports.[28] The PL spectrum peaks at 866 nm, with a Stokes shift of 181nm. This down-conversion coating brings positive affect in two aspects. On the one hand, the higher energy photons tend to produce electron-hole pairs near the surface of device and the photo generated carriers disappear easily through recombination on Si surface with mass of surface defects. Nevertheless, as the PbS QDs down-conversion layer on the front side, the emitted lower energy photons are absorbed in the deeper region, leading to more photons absorbed in the depletion region. With the help of a build-in-electric field, photo-generated electron-hole pairs will be separated immediately and contribute to the J_{sc} enhancement. On the other, in general, one photon just excites single electron-hole pair in bulk c-Si substrate, the photon energy higher than 1.12 eV cools quickly to the band edges by sequential emission of phonons. With the higher energy photons converted into the lower ones, less energy is lost. Moreover, since the PbS has absorption in visible region, which corresponds with the response spectrum of c-Si, the more utilized visible region will probably provide further contribution to the enhanced J_{sc}.

4. Conclusion

In summary, Si NCs and PbS QDs have been composited together and have achieved 30% PCE improvement, compared to its non Si NCs & non PbS QDs capped counterpart. With a certain down-conversion property of PbS QDs, as well as the enhanced light absorption and minority-carrier lifetime. We demonstrate that this large improvement contains two steps: firstly, the light trapping of Si NCs; secondly, the benefits of surface passivation and photon down conversion from PbS QDs. We believe that the combination of appropriate 1-D Si nanostructure and 0-D QDs will find a promising way to obtain high efficiency c-Si solar cell.

Acknowledgment

This work is supported by the Shanghai Science & Technology Committee (12521102501, 11ZR1426500), the first-class discipline construction planning in Shanghai University, PCSIRT (RT1269), the Program of Shanghai Normal University (DZL124) and the Key Laboratory of Resource Chemistry of Ministry of Education of China.

Notes and references：

The Education Ministry Key Lab of Resource Chemistry and Shanghai Key Laboratory of Rare Earth Functional Materials, Department of Chemistry, Shanghai Normal University, Shanghai 200234, People's Republic of China, Fax:+86-21-64322511; +86-21-64324528 E-mail: xibinyu@shnu.edu.cn

References:

1. W. Shockley, H. J. Queisser, *J. Appl. Phys.,* 1961, **32**, 510-519.

2. M. A. Green, *Solar cells: Operating Principles, Technology and System Applications*; The University of New South Wales, Sydney, Australia, 1998.

3. C. Y. Huang, D. Y. Wang, C. H. Wang, Y. T. Chen, Y. T. Wang, Y. T. Jiang, Y. J. Yang, C. C. Chen, Y. F. Chen, *ACS Nano,* 2010, **4**, 5849-5854.

4. X. Y. Guo, H. Li, B. Y. Ahn, E. B. Duoss, K. J. Hsia, J. A. Lewis, R. G. Nuzzo, *P. Natl. Acad. Sci. Usa.,* 2009, **106**, 20149-20154.

5. S. Park, E. Cho, D. Song, G. Conibeer, M. A. Green, *Sol. Energy Mater. Sol. Cells,* 2009, **93**, 684-690.

6. E. Garnett, P. D. Yang, *Nano Lett.,* 2010, **10**, 1082-1087.

7. K. Q. Peng, S. Lee, *Adv. Mater.,* 2011, **23**, 198-215.

8. L. Aarts, van der Ende, B. M., A. Meijerink, *J. Appl.Phys.,* 2009, **106**, 023522.

9. R. T. Wegh, H. Donker, van Loef, E. V. D., K. D. Oskam, *J. Lumin.,* 2000, **87**, 1017-1019.

10. H. G. Zhao, M. Chaker, D. L. Ma, *J. Phys. Chem. C,* 2009, **113**, 6497-6504.

11. H. Choi, J. H. Ko, Y. H. Kim, S. Jeong, *J. Am. Chem. Soc.,* 2013, **135**, 5278-5281.

12. S. H. Jin, D. H. Kim, G. H. Jun, S. H. Hong, S. Jeon, *ACS Nano,* 2013, **7**, 1239-1245.

13. O. Kojima, H. Nakatani, T. Kita, O. Wada, K. Akahane, M. Tsuchiya, *J. Appl. Phys.,* 2008, **103**, 113504.

14. W. A. Tisdale, K. J. Williams, B. A. Timp, D. J. Norris, E. S. Aydil, X. Y. Zhu, *Science,* 2010, **328**, 1543-1547.

15. A. Pandey, P. Guyot-Sionnest, *Science,* 2008, **322**, 929-932.

16. R. T. Ross, A. J. Nozik., *J. Appl. Phys.,* 1982, **53**, 3813.

17. M. C. Beard, *J. Phys. Chem. Lett.,* 2011, **2**, 1282-1288.

18. O. E. Semonin, J. M. uther, S. Choi, H. Y. Chen, J. B. Gao, A. J. Nozik, M. C. Beard, *Science,* 2011, **334**, 1530-1533.

19. D. N. Congreve, J. Y. Lee, N. J. Thompson, E. Hontz, S. R. Yost, P. D. Reusswig, M. E. Bahlke, S. Reineke, T. Van Voorhis, M. A. Baldo, *Science,* 2013, **340**, 334-337.

20. K. Balasundaram, P. K. Mohseni, Y. C. Shuai, D. Y. Zhao, W. D. Zhou, X. L. Li, *Appl. Phys. Lett.,* 2013, **103**, 204103

21. M. Z. Tymieniecki, Z. A. K. Durrani, *Appl. Phys. Lett.,* 2011, **98**, 102113

22. X. Li and P. W. Bohn, *Appl. Phys. Lett.,* 2000, **77**, 2572

23. H. G. Zhao, D. F. Wang, M. Chaker, D. L. Ma, *J. Phys. Chem. C,* 2009, **113**, 6497-6504.

24. K. Q. Peng, Y. Xu, Y. Wu, Y.J. Yan, S. Lee, J. Zhu, *small,* 2005, **11**, 1062-1067.

25. C. Y. Huang, G. C. Lin, Y. J. Wu, T. Y. Lin, Y. J. Yang, Y. F. Chen, *J. Phys. Chem. C,* 2011, **115**, 13083-13087.

26. E. Istrate, S. Hoogland, V. Sukhovatkin, L. Levina, S. Myrskog, P. Smith, E. H. Sargent, *J. Phys. Chem. B,* 2008, **112**, 2757-2760.

27. Y. Yang, W. Rodriguez-Cordoba, T. Q. Lian, *Nano Lett.,* 2012, **12**, 4235-4241.

28. S. Baskoutas, A. F. Terzis, W. Schommers, *J. Comput. Theor. Nanoscience*, 2006, **3**, 269-271.

Figures

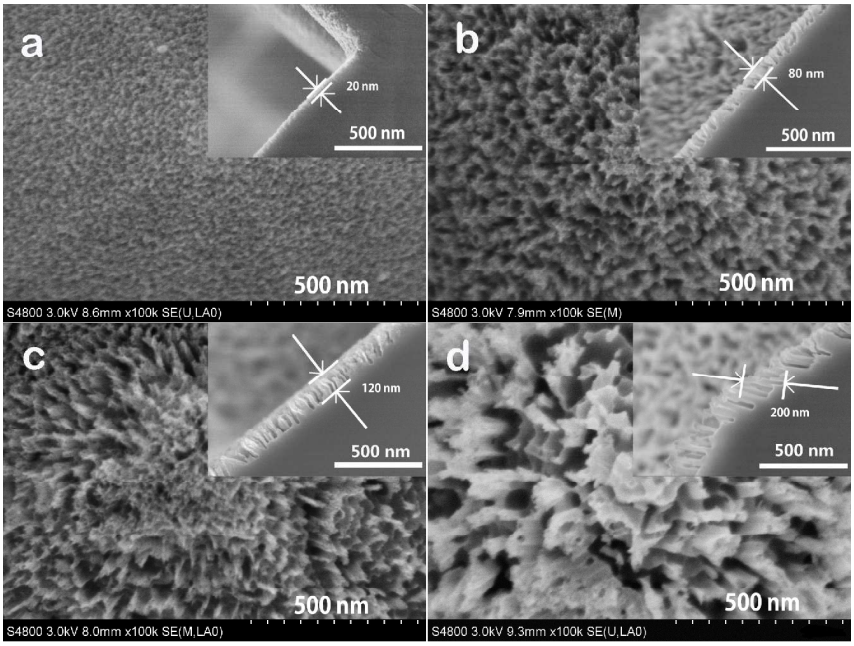

Fig. 1 Surface and cross sectional FESEM images of silicon nanocorals (a) 20 nm, (b) 80 nm, (c) 120 nm, (d) 200 nm.

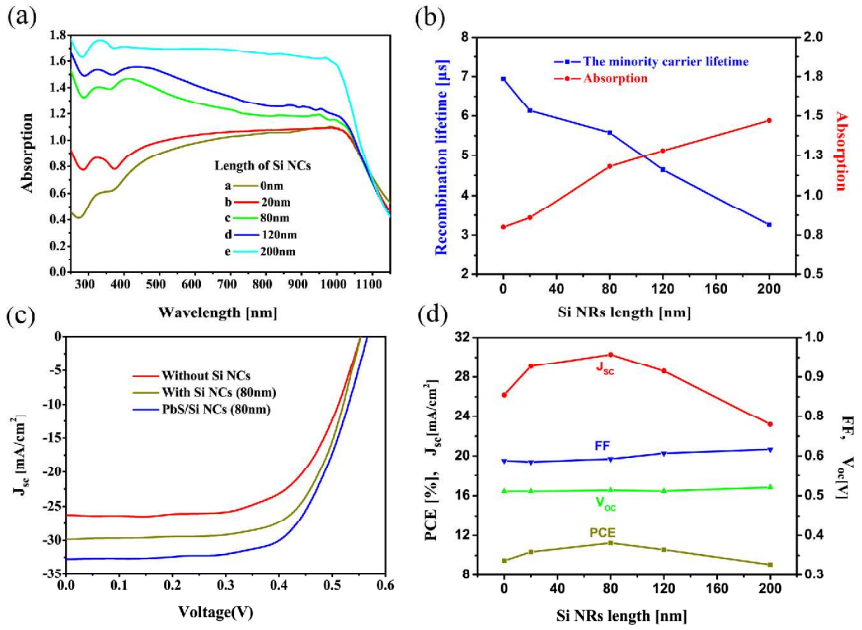

Fig. 2 (a) Absorption spectra of Si NCs solar cells. (b) Effect of the length of Si NCs on effective recombination minority-carrier lifetime and optical absorption spectra of Si NCs solar cells. (c) J-V characteristics of pyramid textured Si without NCs, pyramid textured Si with 80 nm NCs, and the PbS QDs/Si NCs composited solar cell. (d) Effect of the length of Si NCs on J_{sc}, V_{oc}, FF, and PCE of Si NCs solar cells.

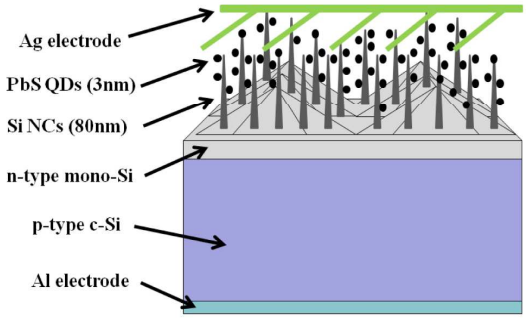

Fig. 3 Schematic illustration of Si NCs/PbS QDs composited solar cell, based on the pyramid textured mono-Si.

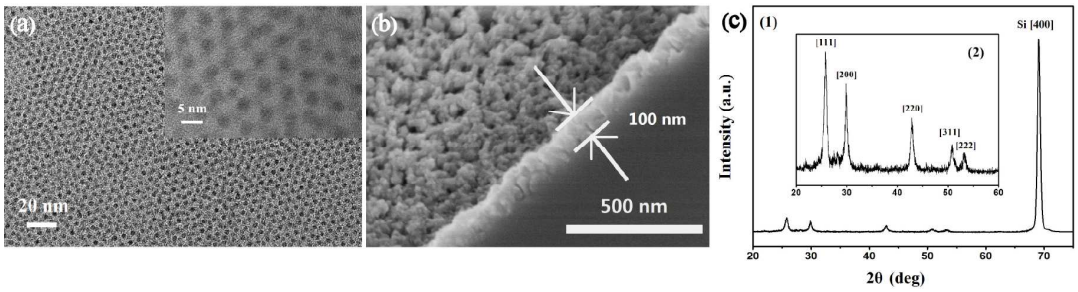

Fig. 4 (a) TEM image of PbS QDs. (b) cross section FESEM image of Si NCs (80 nm) capped with PbS QD. (c) X-ray diffraction pattern of PbS QDs and the composited PbS QDs/ Si NCs solar cell.

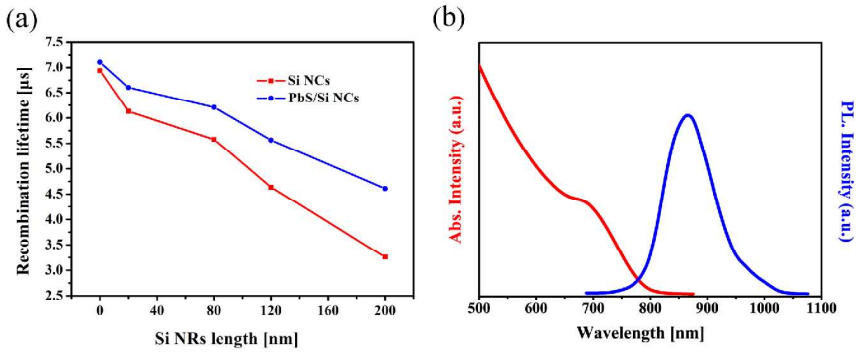

Fig. 5 (a) Effect of the Si NCs length on surface recombination lifetime of Si NCs solar cell and the composited solar cell. (b) Absorption spectra and photoluminescence spectra of PbS QDs.

Table

Tab. 1 Photovoltaic performances of three different Si solar cells.

---	V_{oc} (mV)	J_{sc} (mA/cm^2)	FF (%)	PCE (%)	ΔPCE
Pyramid textured Si	0.548	26.22	66.1	9.49	---
Si NCs (80 nm)	0.551	30.07	67.3	11.15	17.5%
PbS/Si NCs (80nm)	0.566	32.76	66.6	12.34	30.0%

Table of contents

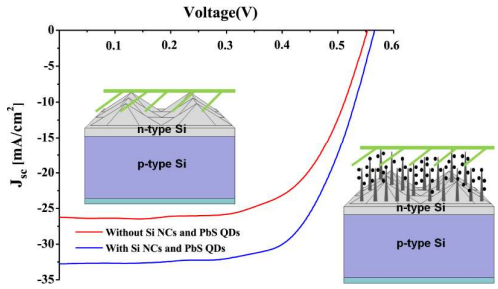

A composited Si nanocorals/PbS quantum dots p-n active layer (with pyramid textured surface) achieved 30% increase in power conversion efficiency.